Supporting Information for

Grafted dipolar chains: Dipoles and restricted freedom lead to unexpected hairpins

*Artyom D. Glova,[†] Sergey V. Larin,[†] Victor M. Nazarychev,[†] Mikko Karttunen,[†, ‡, #, *] and Sergey V. Lyulin[†,*]*

†Institute of Macromolecular Compounds, Russian Academy of Sciences, Bolshoj pr. 31 (V.O.), St. Petersburg 199004, Russia

‡Department of Chemistry and Department of Applied Mathematics, the University of Western Ontario, 1151 Richmond Street, London, Ontario, Canada N6A 5B7

#The Centre of Advanced Materials and Biomaterials Research, the University of Western Ontario, 1151 Richmond Street, London, Ontario, Canada N6A 5B7

**Correspondence to:* s.v.lyulin@gmail.com, mkarttu@uwo.ca

Values of atomic partial charges

Lactide chain

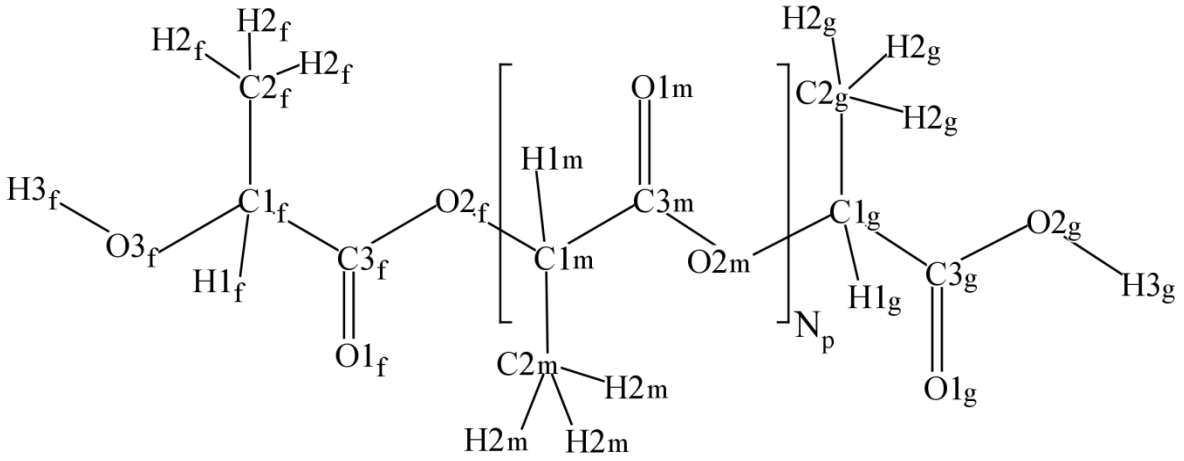

Atom name	Partial charge, e
C1f	0.76
C2f	-0.17
C3f	0.19
O1f	-0.47
O2f	-0.49
O3f	-0.67
H1f	0.08
H2f	0.09
H3f	0.50
C1m	0.22
C2m	-0.30
C3m	0.70
O1m	-0.53
O2m	-0.44
H1m	0.08
H2m	0.09
C1g	0.18
C2g	-0.23
C3g	0.62
O1g	-0.60
O2g	-0.55
H1g	0.02
H2g	0.05
H3g	0.41

Hydroxybutyrate chain

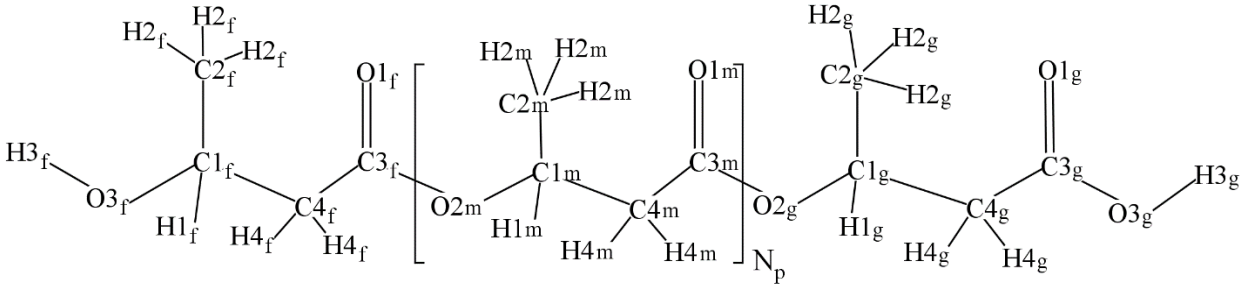

Atom name	Partial charge, e
C1f	0.32
C2f	-0.15
C3f	0.71
C4f	-0.26
O1f	-0.59
O3f	-0.70
H1f	-0.02
H2f	0.05
H3f	0.40
H4f	0.07
C1m	0.32
C2m	-0.35
C3m	0.74
C4m	-0.19
O1m	-0.58
O2m	-0.46
H1m	0.06
H2m	0.10
H4m	0.08
C1g	0.31
C2g	-0.30
C3g	0.75
C4g	-0.16
O1g	-0.59
O2g	-0.43
O3g	-0.60
H1g	0.08
H2g	0.10
H3g	0.48
H4g	0.08

Cellulose chain

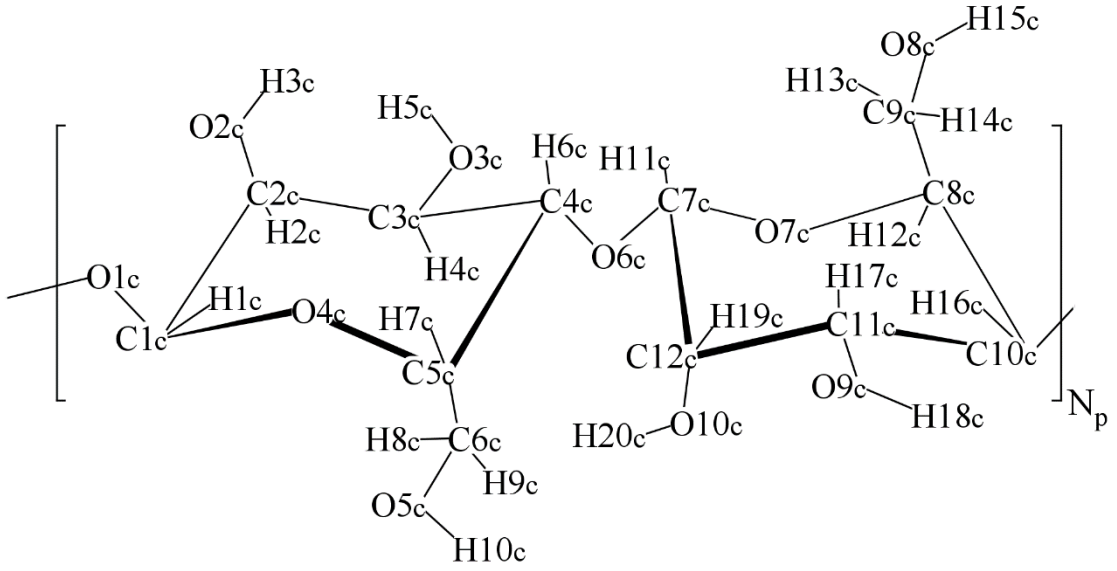

Atom name	Partial charge, e
O1c	-0.32
O2c	-0.62
O3c	-0.61
O4c	-0.34
O5c	-0.64
O6c	-0.32
O7c	-0.34
O8c	-0.64
O9c	-0.61
O10c	-0.62
C1c	0.08
C2c	0.22
C3c	0.11
C4c	0.02
C5c	0.06
C6c	0.13
C7c	0.08
C8c	0.06
C9c	0.13
C10c	0.02
C11c	0.11
C12c	0.22
H1c	0.11
H2c	0.11
H3c	0.41
H4c	0.11
H5c	0.42
H6c	0.11
H7c	0.11
H8c	0.05
H9c	0.05

H10c	0.43
H11c	0.11
H12c	0.11
H13c	0.05
H14c	0.05
H15c	0.43
H16c	0.11
H17c	0.11
H18c	0.42
H19c	0.11
H20c	0.41

Lactide-modified cellulose chain

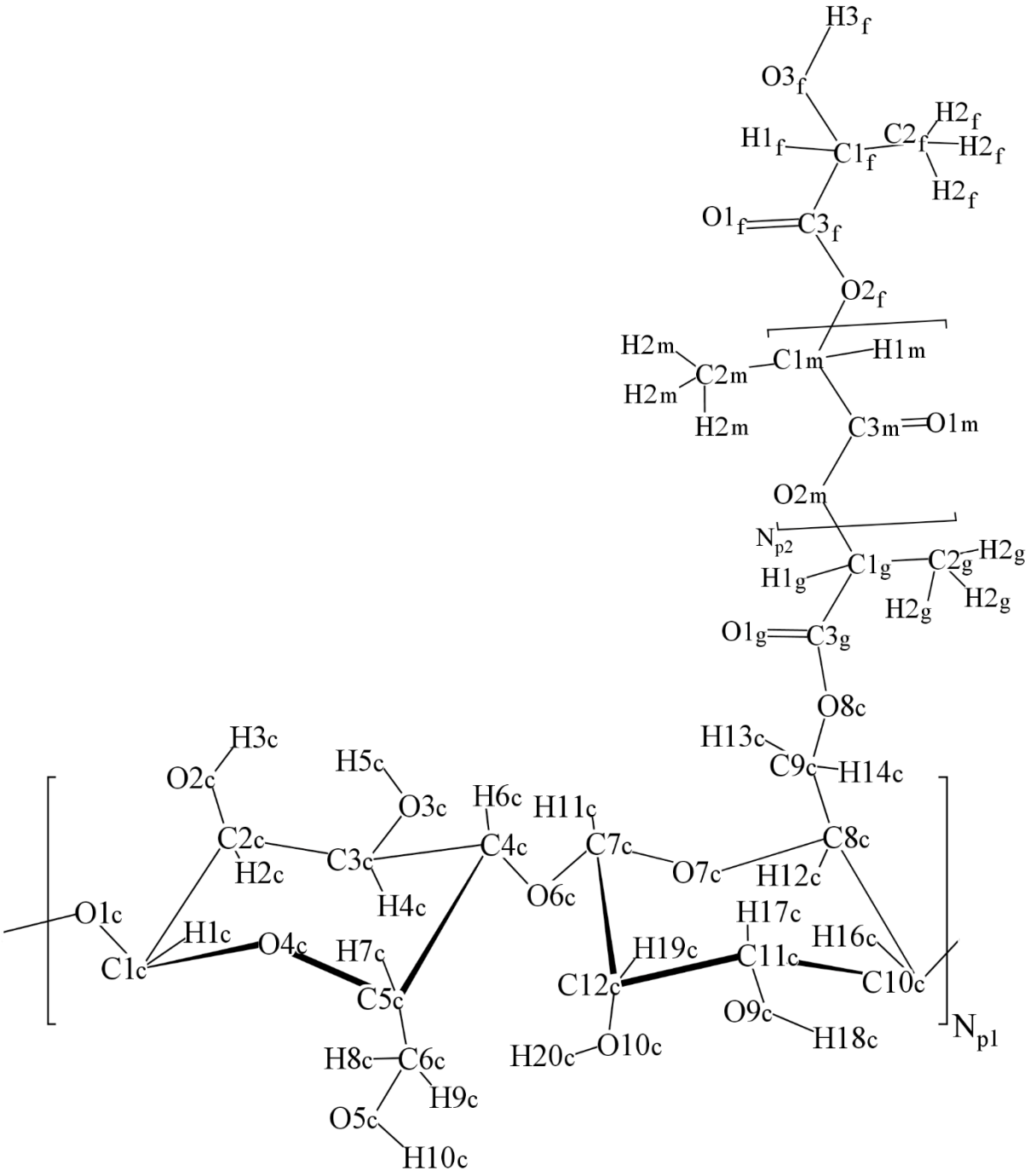

Atom name	Partial charge, e
C1f	0.76
C2f	-0.17
C3f	0.19
O1f	-0.47
O2f	-0.49
O3f	-0.67
H1f	0.08
H2f	0.09
H3f	0.50
C1m	0.22

C2m	-0.30
C3m	0.70
O1m	-0.53
O2m	-0.44
H1m	0.08
H2m	0.09
C1g	0.09
C2g	-0.16
C3g	0.82
O1g	-0.23
H1g	0.09
H2g	0.06
O1c	-0.32
O2c	-0.62
O3c	-0.61
O4c	-0.34
O5c	-0.64
O6c	-0.32
O7c	-0.44
O8c	-0.44
O9c	-0.61
O10c	-0.62
C1c	0.08
C2c	0.22
C3c	0.11
C4c	0.02
C5c	0.06
C6c	0.13
C7c	0.08
C8c	0.04
C9c	0.02
C10c	0.02
C11c	0.11
C12c	0.22
H1c	0.11
H2c	0.11
H3c	0.41
H4c	0.11
H5c	0.42
H6c	0.11
H7c	0.11
H8c	0.05
H9c	0.05
H10c	0.43
H11c	0.11
H12c	0.11
H13c	0.06
H14c	0.06
H16c	0.11
H17c	0.11

H18c	0.42
H19c	0.11
H20c	0.41

Hydroxybutyrate-modified cellulose chain

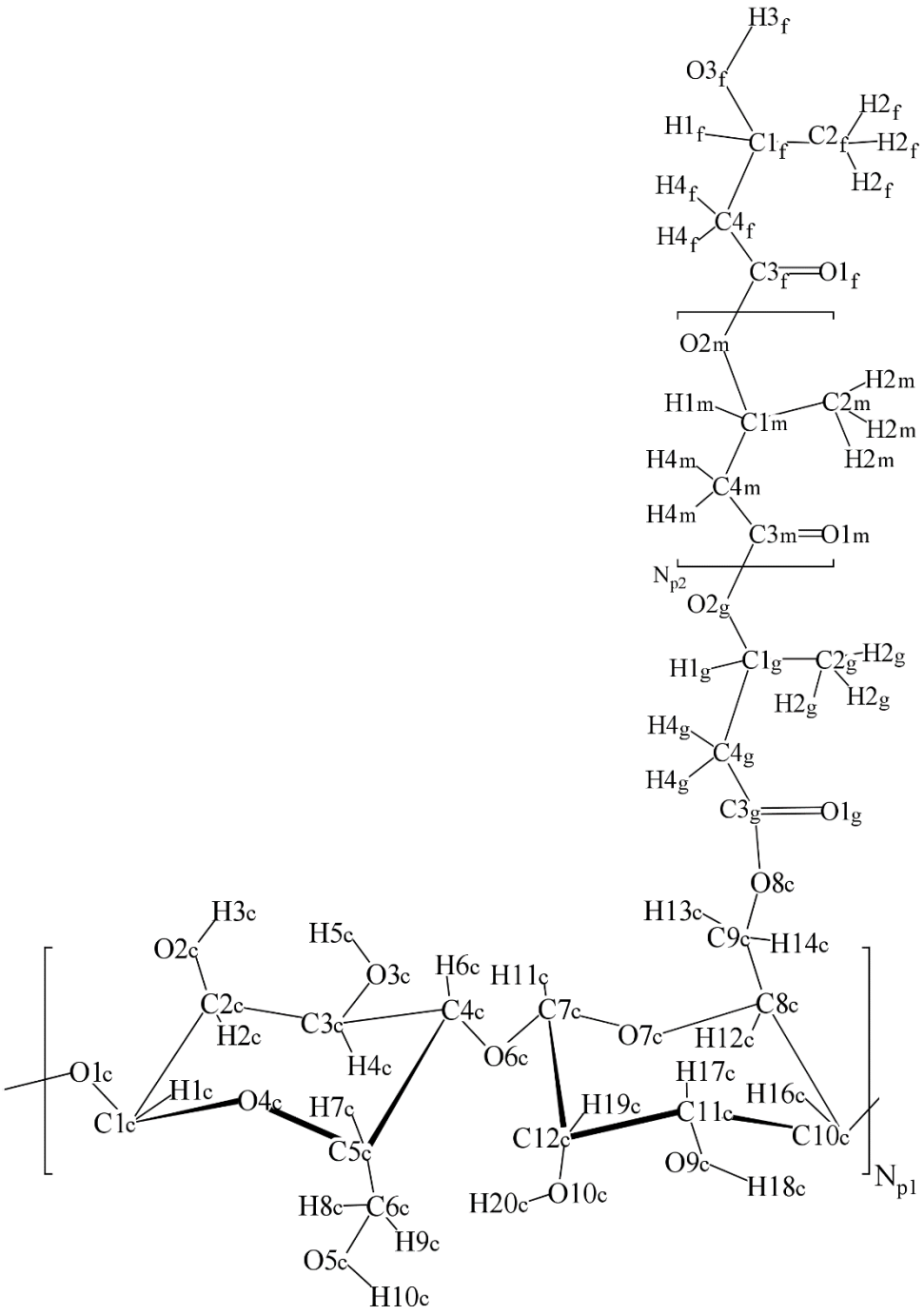

Atom name	Partial charge, e
C1f	0.32
C2f	-0.15
C3f	0.71
C4f	-0.26
O1f	-0.59

O3f	-0.70
H1f	-0.02
H2f	0.05
H3f	0.40
H4f	0.07
C1m	0.32
C2m	-0.35
C3m	0.74
C4m	-0.19
O1m	-0.58
O2m	-0.46
H1m	0.06
H2m	0.10
H4m	0.08
C1g	0.31
C2g	-0.30
C3g	0.82
C4g	-0.16
O1g	-0.59
O2g	-0.43
H1g	0.08
H2g	0.10
H4g	0.08
O1c	-0.32
O2c	-0.62
O3c	-0.61
O4c	-0.34
O5c	-0.64
O6c	-0.32
O7c	-0.34
O8c	-0.44
O9c	-0.61
O10c	-0.62
C1c	0.08
C2c	0.22
C3c	0.11
C4c	0.02
C5c	0.06
C6c	0.13
C7c	0.08
C8c	0.06
C9c	0.15
C10c	0.02
C11c	0.11
C12c	0.22
H1c	0.11
H2c	0.11
H3c	0.41
H4c	0.11
H5c	0.42

H6c	0.11
H7c	0.11
H8c	0.05
H9c	0.05
H10c	0.43
H11c	0.11
H12c	0.11
H13c	0.06
H14c	0.06
H15c	0.43
H16c	0.11
H17c	0.11
H18c	0.42
H19c	0.11
H20c	0.41

Distribution of free ends of grafted OLA chains $p(Z_e)$ in the GAFF and PLAFF3 force fields

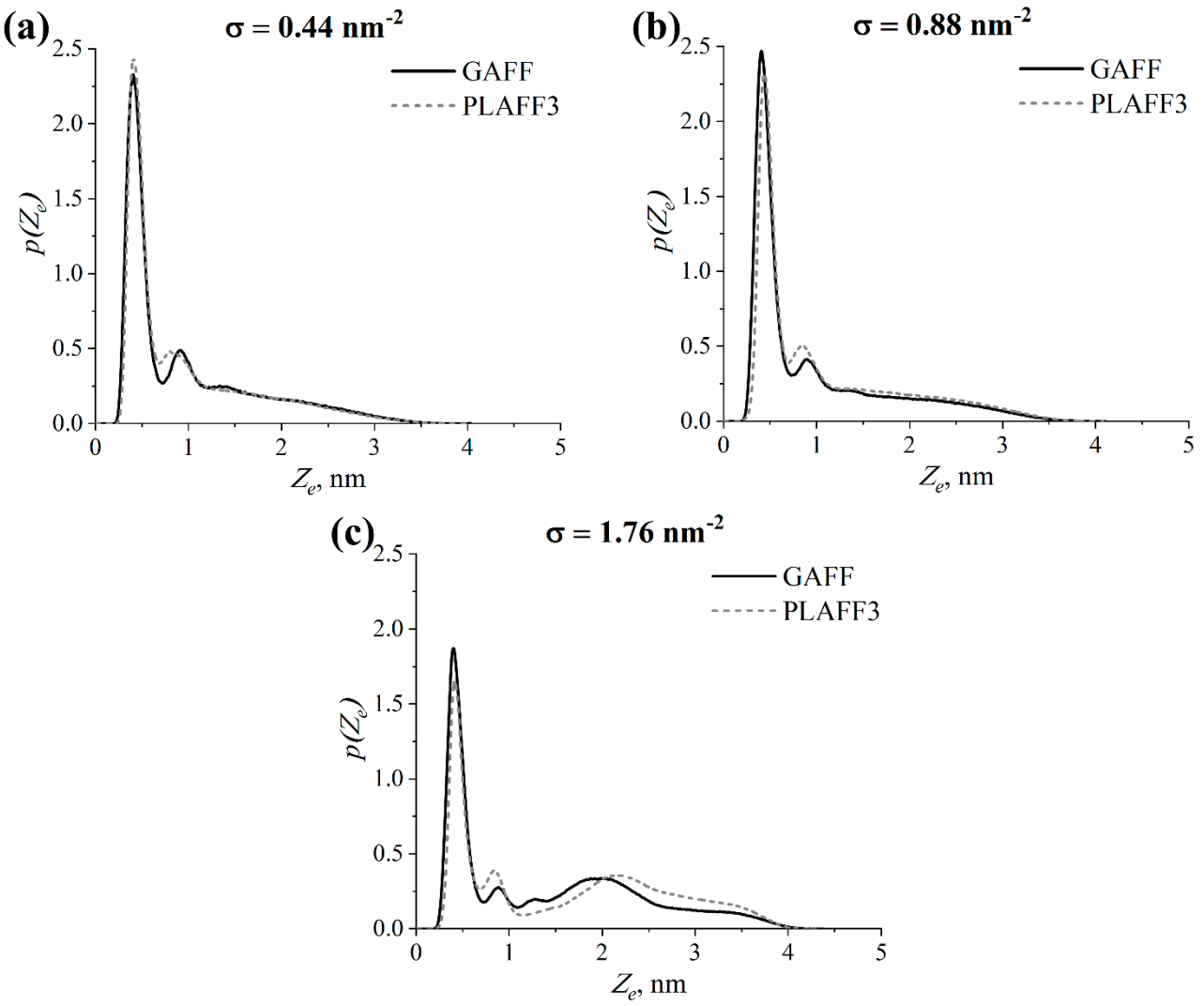

Figure S1. Distribution of free ends of the grafted OLA chains $p(Z_e)$ with respect to the CNC surface at various grafting densities σ in the systems parametrized using the GAFF[1] and PLAFF3[2] force fields. Note that both force fields provide consistent results.

Starting configurations of surface-modified cellulose nanocrystals and composites

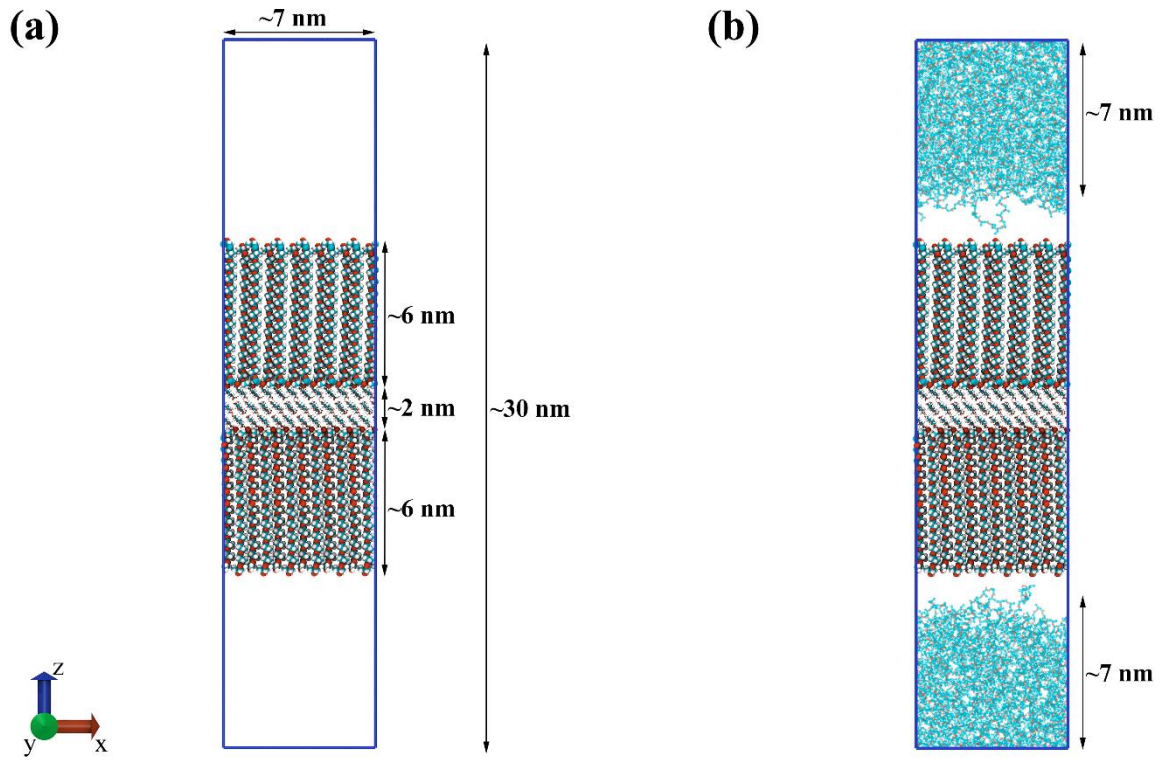

Figure S2. Snapshots of starting configurations of (a) modified cellulose nanocrystals with vertically oriented grafted OHB chains and (b) the corresponding PHB-based composite in the case of the grafting density σ = 1.76 nm^{-2}. Carbons, oxygens and hydrogens are colored in cyan, red and white, respectively. For visual clarity, PHB and OHB chains are drawn by lines and van der Waals spheres, respectively; cellulose chains are shown in the ball and stick representation. Typical dimensions of the system components are indicated by black arrows.

Bivariate joint probability distribution $P(Z_e|H_{end\text{-}to\text{-}end})$ the OHB and OLA chains

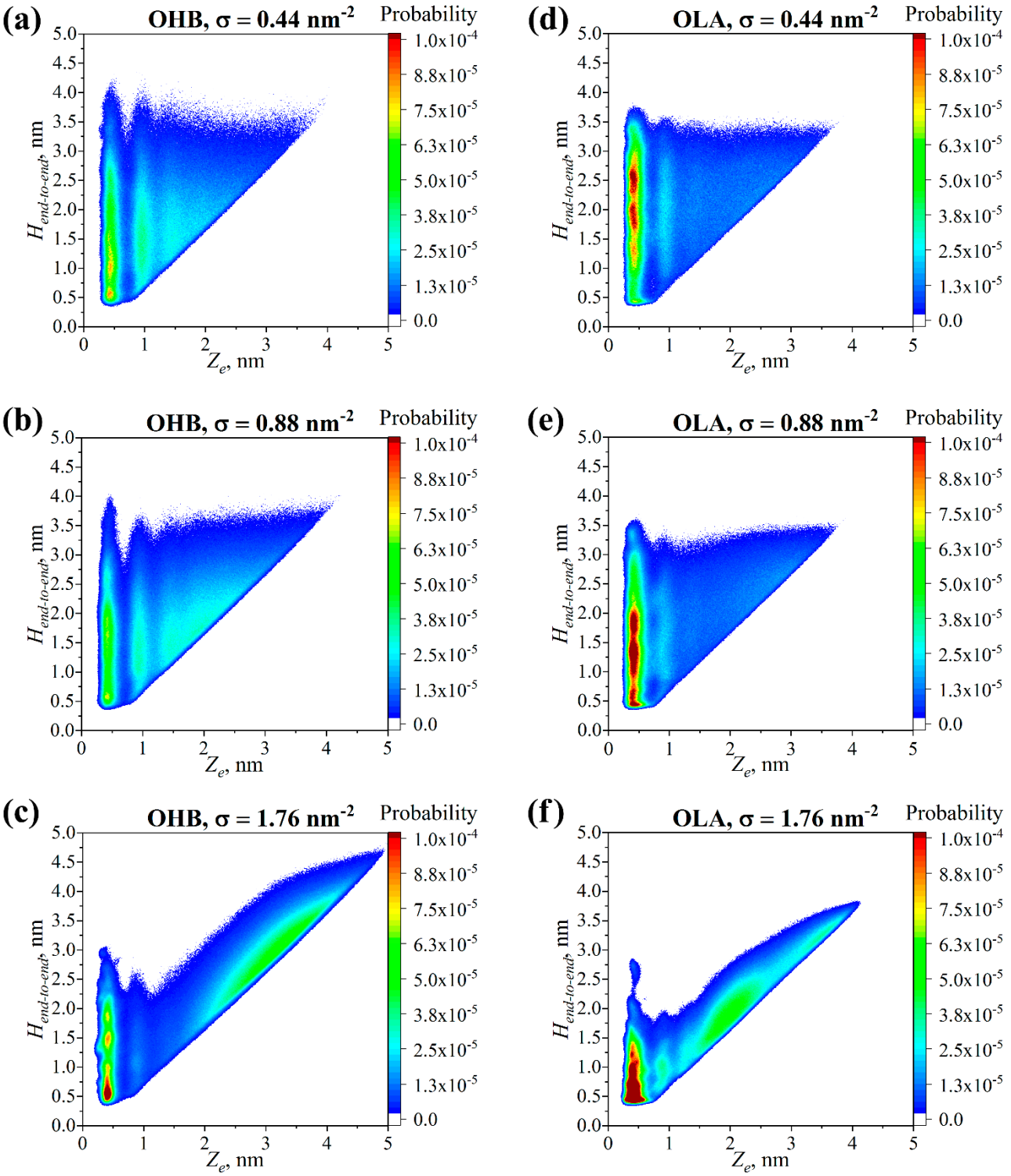

Figure S3. Bivariate joint probability distributions $P(Z_e|H_{end\text{-}to\text{-}end})$, where Z_e is the z coordinate of a terminal carbon atom of a graft with respect to the CNC surface and $H_{end\text{-}to\text{-}end}$ is the end-to-end distance of the graft in the case of the (a-c) OHB and (d-f) OLA chains in the systems with different grafting densities σ.

Definition of parameters for the calculation of the intermolecular interaction energy

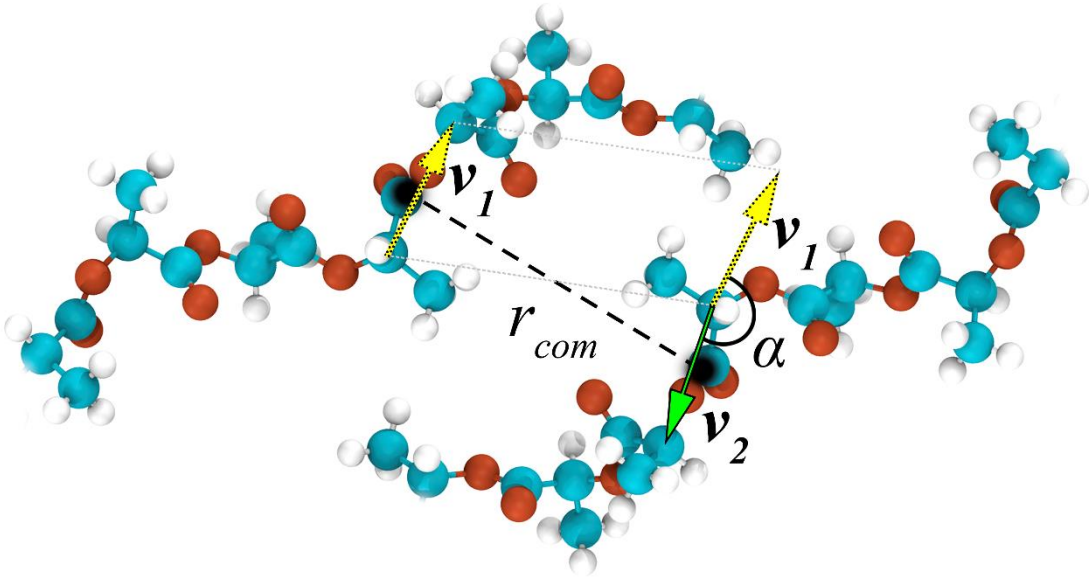

Figure S4. Definition of the center of mass distance r_{com} between the monomers of neighboring grafts and the angle α between the vectors of these monomers connecting adjacent chiral atoms along the grafts contour for the calculation of the intermolecular interaction energy $E(r_{com}|\alpha)$.

Intermolecular interaction energy between the OHB or OLA monomers (σ = 0.44 nm^{-2})

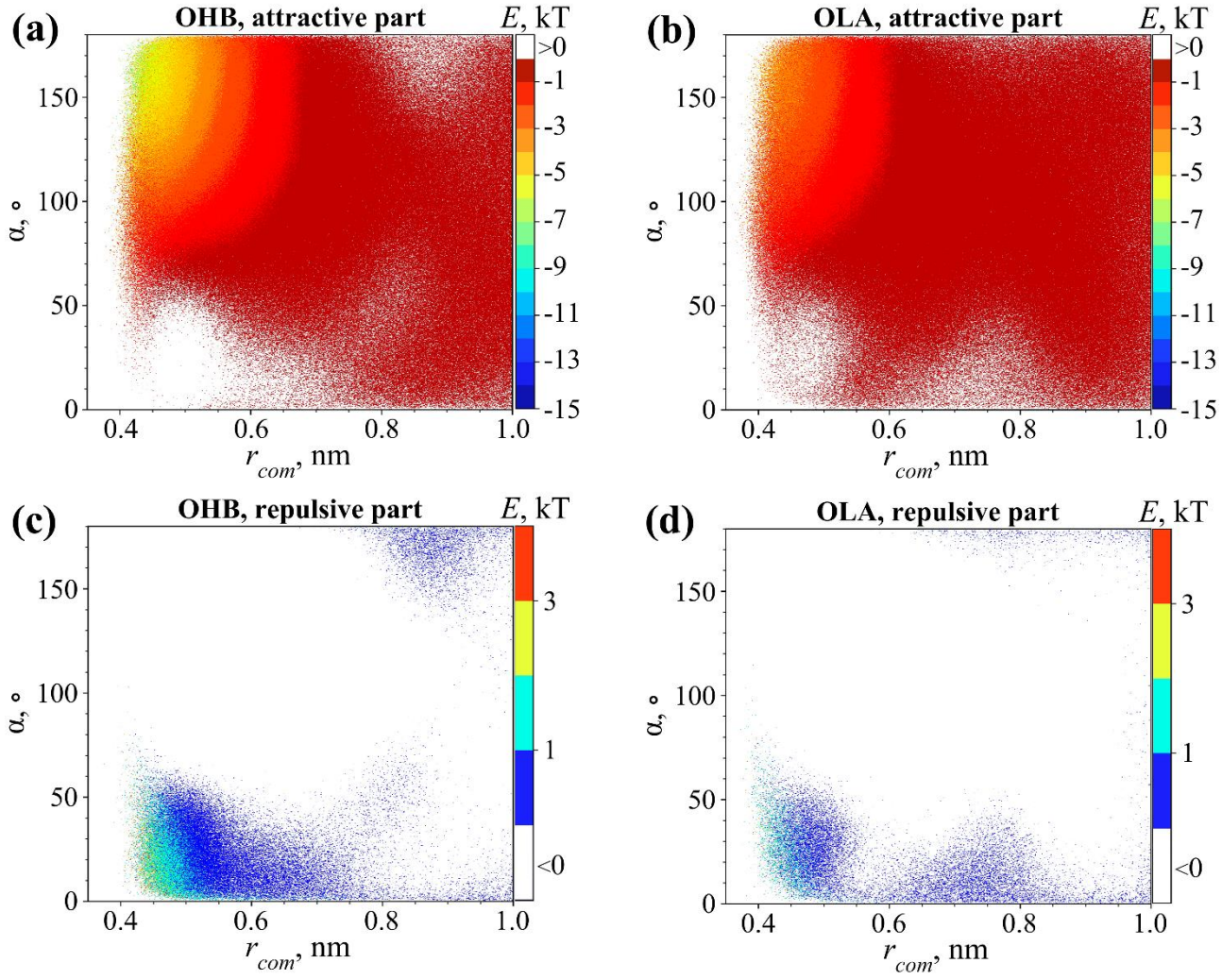

Figure S5. (a, b) Attractive and (c, d) repulsive parts of the intermolecular interaction energy $E(r_{com}|\alpha)$ as a function of distance from centers of masses r_{com} of monomers of neighboring grafts and the angle α between the vectors for these monomers connecting adjacent chiral atoms along the grafts contour in the grafted layer of (a, c) the OHB chains and (b, d) the OLA chains at σ = 0.44 nm^{-2}.

Intermolecular interaction energy between the OHB or OLA monomers (σ = 1.76 nm^{-2})

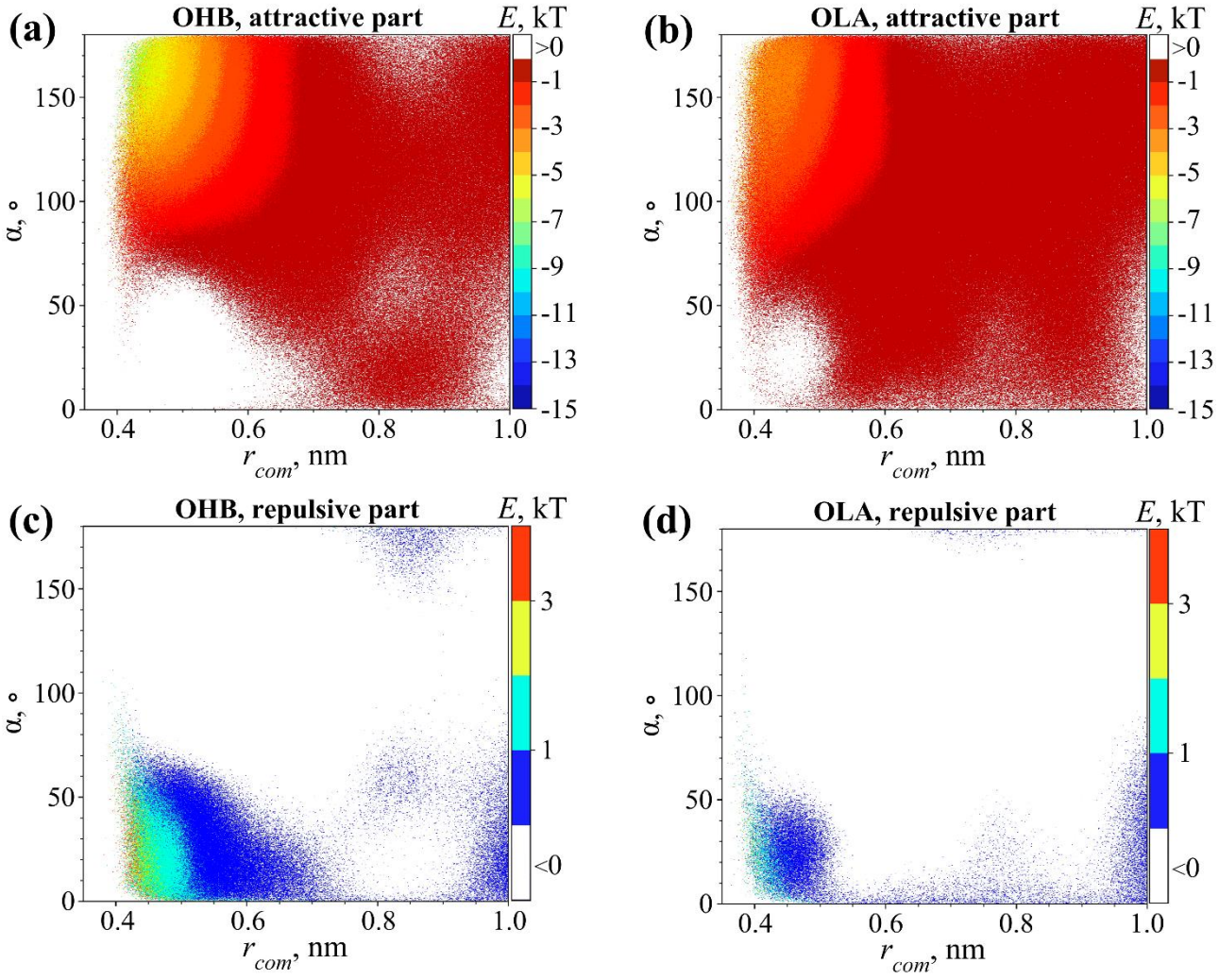

Figure S6. (a, b) Attractive and (c, d) repulsive parts of the intermolecular interaction energy $E(r_{com}|\alpha)$ as a function of distance from centers of masses r_{com} of monomers of neighboring grafts and the angle α between the vectors for these monomers connecting adjacent chiral atoms along the grafts contour in the grafted layer of (a, c) the OHB chains and (b, d) the OLA chains at σ = 1.76 nm^{-2}.

Coulomb contribution to intermolecular interaction energy between the OHB or OLA monomers (σ = 0.88 nm^{-2})

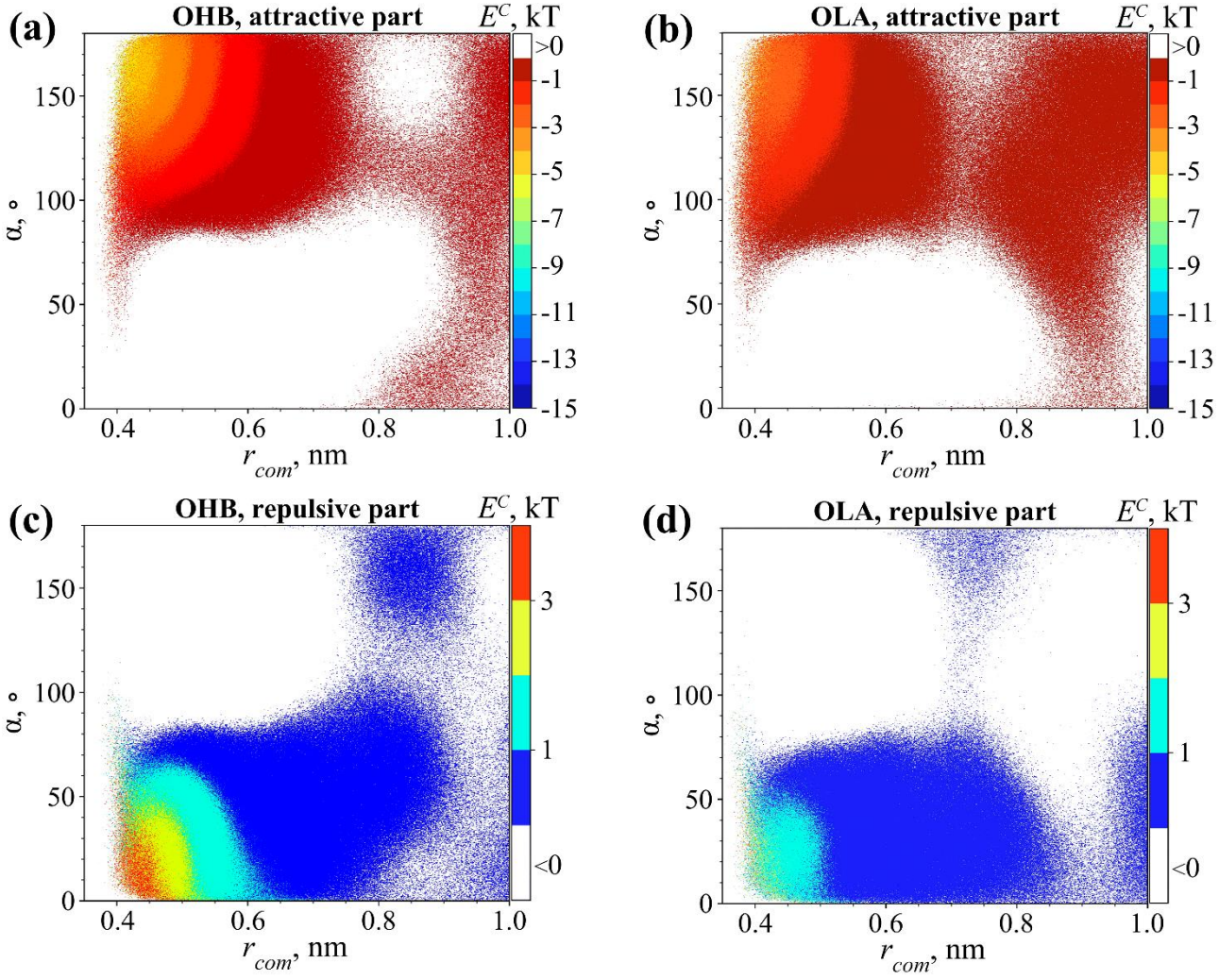

Figure S7. (a, b) Attractive and (c, d) repulsive parts of the Coulomb contribution to the intermolecular interaction energy $E^C(r_{com}|\alpha)$ as a function of distance from centers of masses r_{com} of monomers of neighboring grafts and the angle α between the vectors for these monomers connecting adjacent chiral atoms along the grafts contour in the grafted layer of (a, c) the OHB chains and (b, d) the OLA chains.

Lennard-Jones contribution to intermolecular interaction energy between the OHB or OLA monomers (σ = 0.88 nm^{-2})

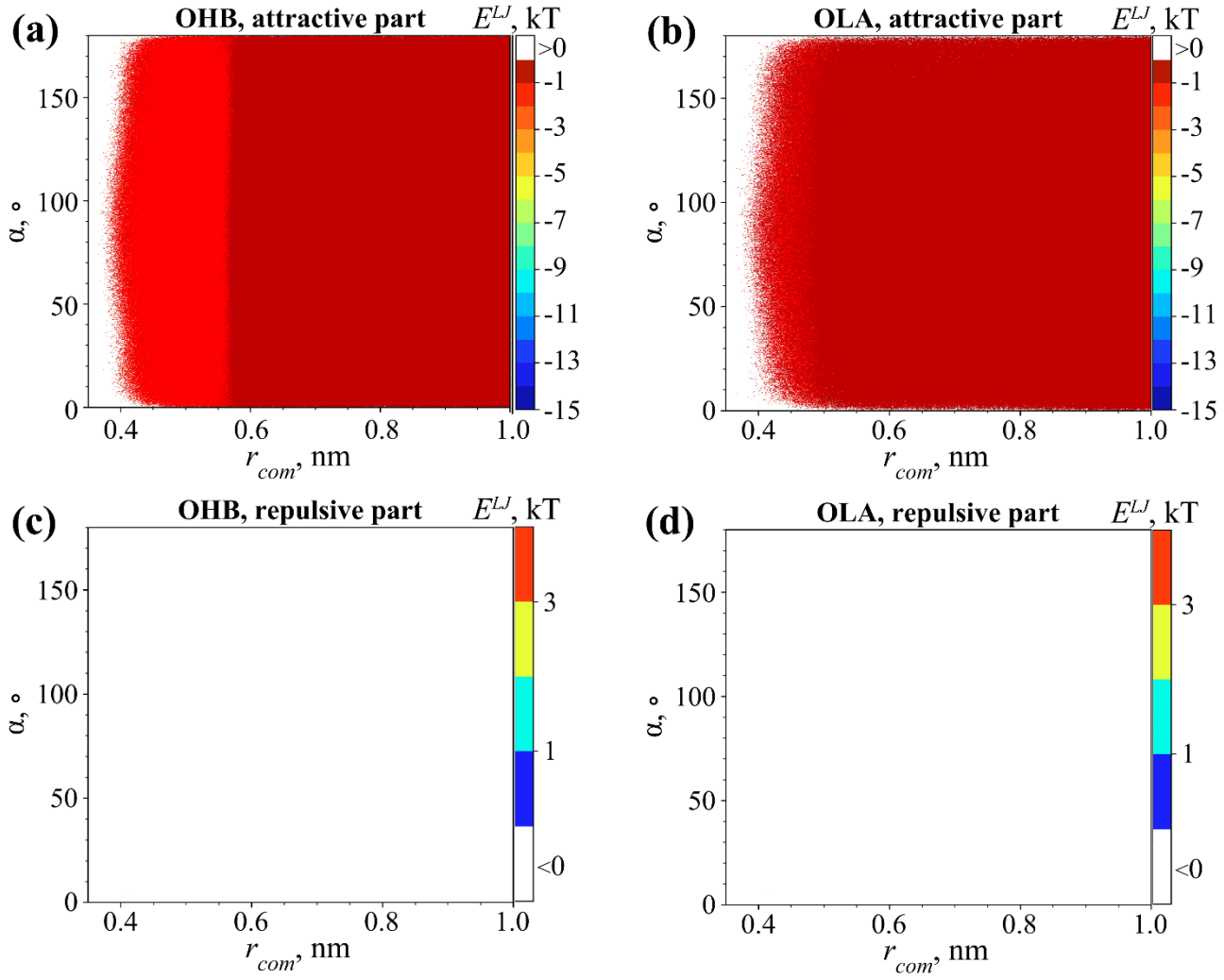

Figure S8. (a, b) Attractive and (c, d) repulsive parts of the Lennard-Jones contribution to the intermolecular interaction energy $E^{LJ}(r_{com}|\alpha)$ as a function of distance from centers of masses r_{com} of monomers of neighboring grafts and the angle α between the vectors for these monomers connecting adjacent chiral atoms along the grafts contour in the grafted layer of (a, c) the OHB chains and (b, d) the OLA chains.

Intramolecular interaction energy between the OHB or OLA monomers (σ = 0.88 nm^{-2})

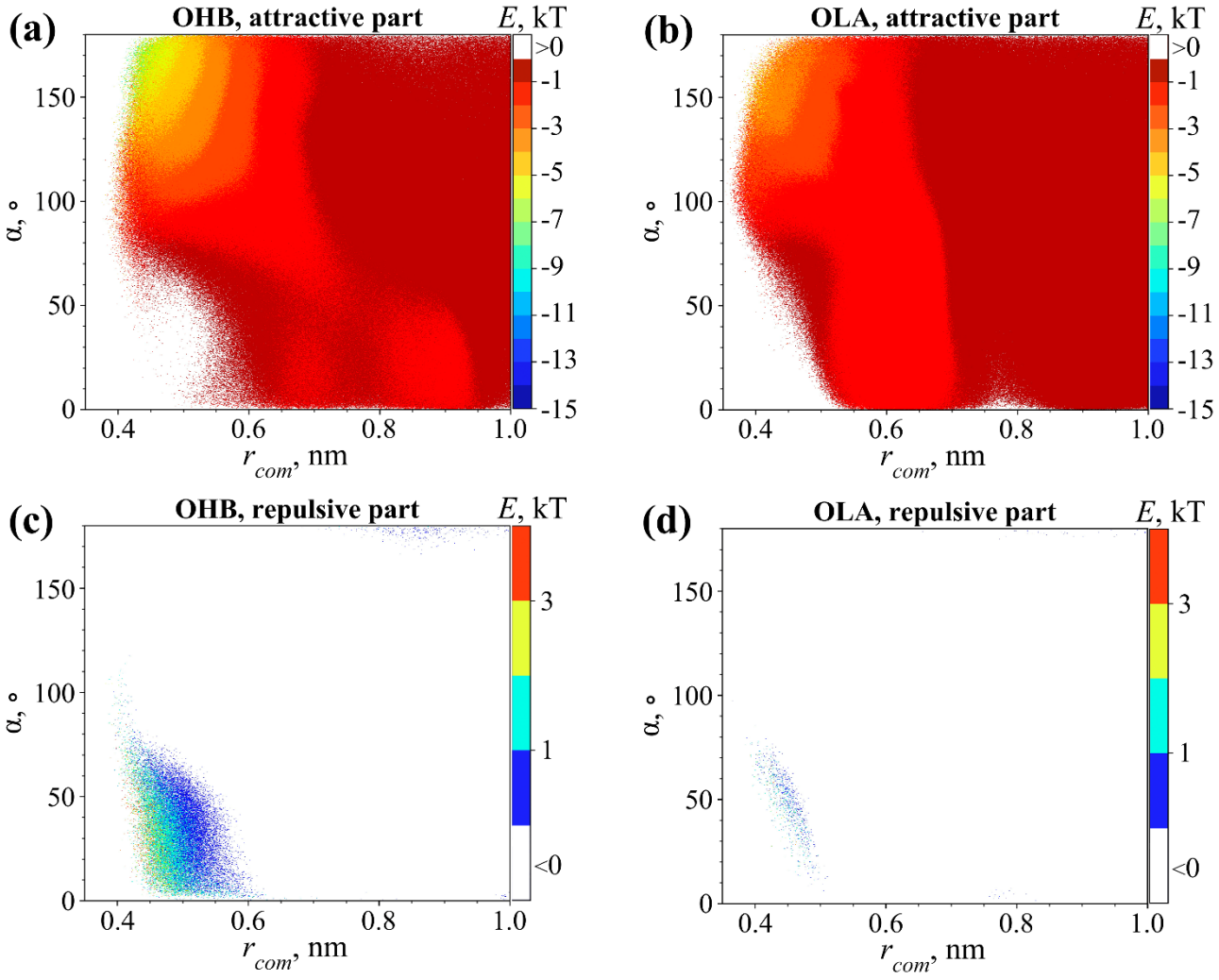

Figure S9. (a, b) Attractive and (c, d) repulsive parts of the intramolecular interaction energy $E(r_{com}|\alpha)$ as a function of distance from centers of masses r_{com} of monomers of within grafts and the angle α between the vectors for these monomers connecting adjacent chiral atoms along the grafts contour in the grafted layer of (a, c) the OHB chains and (b, d) the OLA chains.

Coulomb contribution to intramolecular interaction energy between the OHB or OLA monomers (σ = 0.88 nm^{-2})

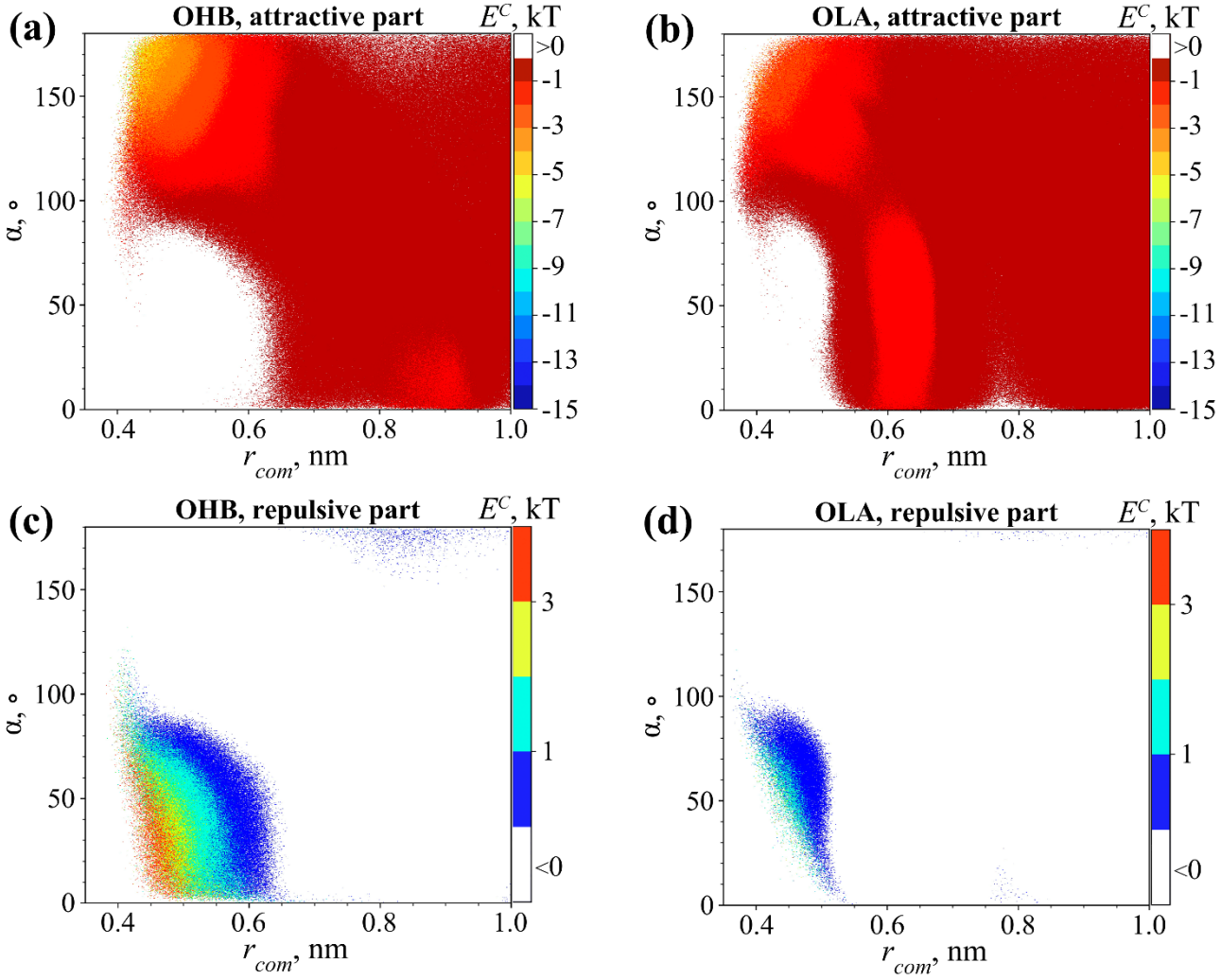

Figure S10. (a, b) Attractive and (c, d) repulsive parts of the Coulomb contribution to the intramolecular interaction energy $E^C(r_{com}|\alpha)$ as a function of distance from centers of masses r_{com} of monomers of within grafts and the angle α between the vectors for these monomers connecting adjacent chiral atoms along the grafts contour in the grafted layer of (a, c) the OHB chains and (b, d) the OLA chains.

Lennard-Jones contribution to intramolecular interaction energy between the OHB or OLA monomers (σ = 0.88 nm^{-2})

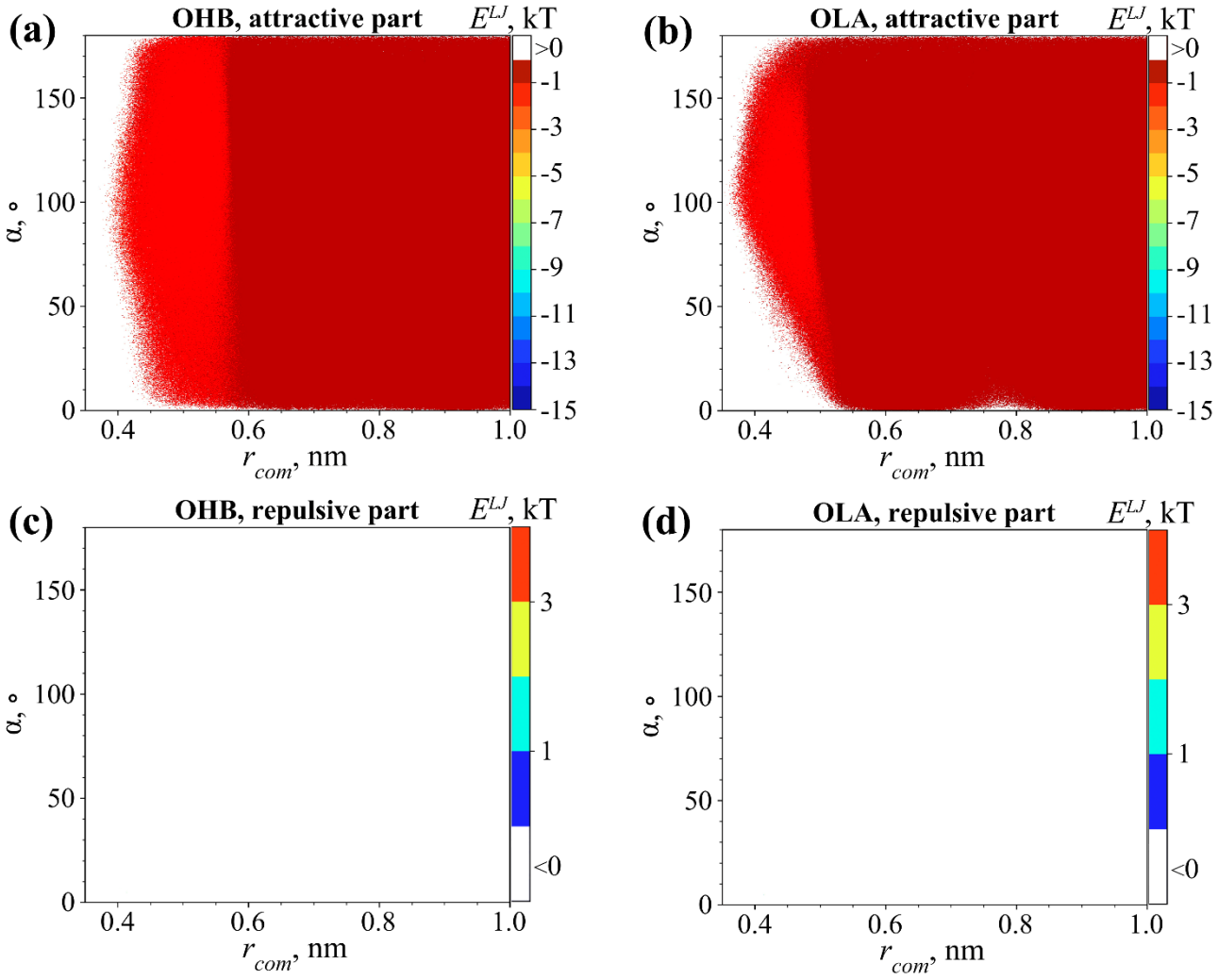

Figure S11. (a, b) Attractive and (c, d) repulsive parts of the Lennard-Jones contribution to the intramolecular interaction energy $E^{LJ}(r_{com}|\alpha)$ as a function of distance from centers of masses r_{com} of monomers of within grafts and the angle α between the vectors for these monomers connecting adjacent chiral atoms along the grafts contour in the grafted layer of (a, c) the OHB chains and (b, d) the OLA chains.

Calculation of the persistence length

To calculate the persistence length of the PLA chains without partial charges and the freely rotating PLA chains, we evaluated the characteristic ratio C_N defined as[3]

$$C_N = \left\langle \frac{R^2(N)}{N \cdot l_b^2} \right\rangle, \quad (1)$$

where $R^2(N)$ is the square distance between two monomers of a chain separated by N chemical bonds, l_b is the mean length of the backbone bond, and the angular brackets indicate an average over all the chains in the system.

Figure S12 shows the obtained C_N dependence on the inverse number $1/N$ of backbone chemical bonds.

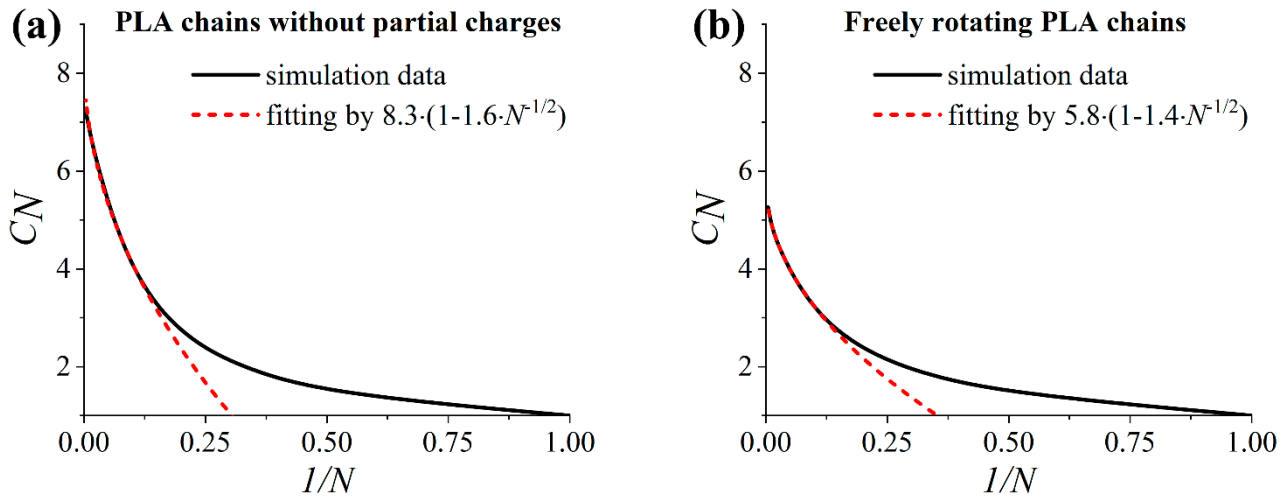

Figure S12. The dependence of the characteristic ratio C_N on the inverse number $1/N$ of the backbone chemical bonds for (a) the PLA chains without partial charges and (b) the freely rotating PLA chains. The solid line indicates the dependence calculated using the simulation trajectory, dashed – the approximation using Eq. 2.

The C_N dependence was used to calculate the characteristic ratio C_∞ of an infinite chain as[3]

$$C_N = C_\infty \cdot \left(1 - \alpha \cdot N^{-1/2}\right), \quad (2)$$

where N is the number of backbone chemical bonds and α is the fitting parameter.

The fitting of the C_N dependence using Eq. 2 yields the values of the characteristic ratio $C_\infty = 8.3 \pm 0.1$ and 5.8 ± 0.1 for the PLA chains without partial charges and the freely rotating PLA chains, respectively.

Thus, the persistent length l_p can be calculated as[4]

$$l_p = \frac{l_b \cdot \left(C_\infty + 1\right)}{2}, \quad (3)$$

The value of the mean bond length of PLA is equal to $l_b = 0.143$ nm according to the parameters of the force field. Therefore, one can find that the value of the persistent length is equal to 0.7 ± 0.1 nm and 0.5 ± 0.1 nm for the PLA chains without partial charges and the freely rotating PLA chains, respectively.

References

(1) Wang, J.; Wolf, R. M.; Caldwell, J. W.; Kollman, P. A.; Case, D. A. Development and Testing of a General Amber Force Field. *J. Comput. Chem.* **2004**, *25* (9), 1157–1174. https://doi.org/10.1002/jcc.20035.

(2) McAliley, J. H.; Bruce, D. A. Development of Force Field Parameters for Molecular Simulation of Polylactide. J. Chem. Theory Comput. 2011, 7 (11), 3756–3767. https://doi.org/10.1021/ct200251x.

(3) Hudzinskyy, D.; Lyulin, A. V.; Baljon, A. R. C.; Balabaev, N. K.; Michels, M. A. J. Effects of Strong Confinement on the Glass-Transition Temperature in Simulated Atactic Polystyrene Films. *Macromolecules* **2011**, *44* (7), 2299–2310 DOI: 10.1021/ma102567s.

(4) Flory, P. J. *Statistical Mechanics of Chain Molecules*; Interscience Publishers: New York, 1969.